sustainability

MDPI

Article

Exploring the Sustainable Development Strategy of Wood Flour-Based Composite Materials in Outdoor Furniture

Huidi Zhou †, Yuqi Gao † and Kaili Zhang *

College of Landscape Architecture, Beijing Forestry University, Beijing 100083, China; gaoyuqi@bjfu.edu.cn (Y.G.)
* Correspondence: zhangkl@bjfu.edu.cn
† These authors contributed equally to this work.

Abstract

Wood flour, a landscaping byproduct, poses disposal challenges due to its poor degradability, despite its potential as a sustainable material. This study modified wood powder by synergistically incorporating fly ash and TiO_2, followed by curing it with polyamide and epoxy resin to produce high-performance wood powder-based composites suitable for outdoor furniture applications, it can solve the environmental problems caused by fly ash. The research findings indicated that as the TiO_2 content increased, the material's pore size diminished, structural strength improved, and it demonstrated enhanced hydrophobic properties and UV absorption capabilities. The optimal UV absorption performance was observed at a TiO_2 content of 1.5%. The combination of TiO_2 and fly ash led to the formation of more stable Si-O-Ti and Si-O-Si bonds, which further strengthened the material. Water contact angle and water repellency tests indicated that the 1.5% TiO_2 composite showed a 12% increase in compressive strength and a water contact angle of 100.6°, indicating improved hydrophobicity. The addition of TiO_2 reduced the number of free-OH groups within the matrix, thereby improving the composite's hydrophobicity. Outdoor chairs fabricated by mixing 1.5% TiO_2-modified wood powder with PET for demolding exhibited excellent structural stability while also being safe and environmentally friendly. This study proposes a feasible preparation strategy for wood powder, enhancing durability through improved mechanical strength, water repellency, and UV shielding. Furthermore, it offers valuable insights into the material modification of wood powder-based materials for the production of outdoor garden furniture.

Keywords: wood flour modification; high strength; UV absorption; hydrophobicity; outdoor furniture

check for updates

Academic Editors: Yanchen Li, Chenglong Zhang, Yanhong Jia and Kaibao Wang

Received: 15 September 2025
Revised: 13 October 2025
Accepted: 14 October 2025
Published: 17 October 2025

Citation: Zhou, H.; Gao, Y.; Zhang, K. Exploring the Sustainable Development Strategy of Wood Flour-Based Composite Materials in Outdoor Furniture. *Sustainability* **2025**, *17*, 9235. https://doi.org/10.3390/su17209235

Copyright: © 2025 by the authors. Licensee MDPI, Basel, Switzerland. This article is an open access article distributed under the terms and conditions of the Creative Commons Attribution (CC BY) license (https://creativecommons.org/licenses/by/4.0/).

1. Introduction

Wood flour is a common biomass waste generated in landscaping. It is rich in cellulose and lignin and can serve as one of the few non-petroleum aromatic carbon sources [1]. This material is not only inexpensive but also environmentally friendly [2]. However, it is difficult for the material to degrade naturally.

Some researchers have developed methods to decompose lignin by designing easily cleavable bonds in the main chain of lignin polymers [3]. Nevertheless, the vast majority of wood powder is either incinerated as low-value fuel or sent to landfills [4,5], causing significant environmental pollution. Therefore, finding high-value applications for lignocellulosic biomass is critical not only for reducing carbon dioxide emissions but also for addressing the degradation challenges associated with the accumulation of solid waste [6,7]. Currently,

the utilization of wood powder-based composite materials in the production of outdoor garden furniture can effectively mitigate the difficulties in processing wood powder [8]. Additionally, the acquisition of wood powder is both convenient and rapid, aligning with the goals of low carbon emissions and environmental protection.

While outdoor furniture made from wood powder is aesthetically pleasing, natural, and environmentally friendly, it inevitably faces challenges such as susceptibility to decay, oxidation, and poor stability [9], which shorten its service life. Prolonged exposure to outdoor conditions significantly diminishes its overall performance, leading to issues such as cracking, deformation, fading, aging due to ultraviolet radiation, and surface peeling [10,11]. Consequently, enhancing the light aging resistance and mechanical strength of wood powder-based materials has become a focal point of research in outdoor furniture applications. To improve the mechanical properties of wooden furniture, researchers have conducted extensive studies, including the addition of preservatives to wood powder and the use of ball-milled graphene to reduce fiber size and increase specific surface area for wood modification [12,13]. These improvements primarily arise from the introduction of new functional groups and physical treatment methods aimed at enhancing the mechanical properties and stability of wooden furniture. However, long-term exposure to light can still lead to the aging and degradation of glycosidic bonds in wood fibers, resulting in a significant reduction in strength [14]. Therefore, appropriate modification methods are necessary to further enhance the strength of wood powder-based composite materials. At the molecular level, Donath et al. [15] utilized alkoxysilane and hydroxyl groups in wood cellulose as reaction sites to modify wood, resulting in the formation of more stable Si-O-Si bonds, which improved the material's performance. Mosadeghzada et al. [16] mixed 10% NaOH-treated wood powder with unsaturated polyester resin (UPR) to enhance the bonding between the materials, thereby improving the mechanical properties of the mixture through surface treatment and filler loading. Novosel et al. [17] incorporated carbon fiber into pressed wood boards. By leveraging the high tensile strength of carbon fiber, they created local bridge-like connections that reduced bending deformation, consequently increasing the effective stiffness (EI) of the board by 4% to 94% and the ultimate failure load (ULF) by 2% to 106%. Furthermore, fly ash, another type of solid waste that has not been extensively recycled, is commonly utilized for reinforcing and modifying composite materials. Its main components are SiO_2 and Al_2O_3 [18,19]. The controllable porosity, thermal stability, and chemical inertness of SiO_2 render it a highly stable, acid- and alkali-resistant non-metallic oxide [20]. Fly ash can improve the mechanical strength and stability of wood materials, thus achieving reinforcement and modification. Zygmunt et al. [19] applied modified fly ash to polyurethane foam to enhance the applicability of composite materials, with the modified fly ash polyurethane material silanized with 1% and 2% silane solutions demonstrating optimal performance. Cao et al. [21] introduced SiO_2 coatings to improve the hydrophobicity of wood, thus enhancing the overall strength of the substrate. While wood flour composites have been explored, few studies have addressed their simultaneous mechanical, UV, and water resistance limitations using industrial waste materials. The fly ash produced by industry can generate dust, pollute the atmosphere, and pose great harm to human health and the environment. Therefore, using fly ash to modify wood powder can not only improve the performance of composite materials, but also solve the environmental problems caused by fly ash.

In addition to improving mechanical strength, wood powder-based materials also need to exhibit strong resistance to photooxidation. However, conventional chemical and thermal treatment methods are often insufficient in preventing the oxidation of wood furniture due to poor photodegradation when exposed to UV and visible light [22]. Common UV-protective coatings include organic absorbers such as benzophenone [23] and inorganic

absorbers like TiO_2 and ZnO [24–26]. Miloš et al. [27] prepared a transparent coating using caffeine and TiO_2 nanoparticles that effectively resists UV radiation and mold erosion. Ghamarpoor et al. [28] investigated the impact of TiO_2 nanoparticles of varying sizes on UV protection, demonstrating that titanium dioxide can filter all types of UVA and UVB rays. Bulcha et al. [29] treated cotton textiles with zinc oxide nanoparticles, improving their ultraviolet protection factor (UPF). Benzophenone and its derivatives have also been frequently employed to filter ultraviolet radiation [30]. In contrast, TiO_2 exhibits high chemical stability and an excellent UV absorption capacity. Moreover, the active free radicals generated by light exposure can exert antibacterial effects [31–33]. Consequently, TiO_2 serves as an outstanding modification material for enhancing the photooxidation resistance and UV-shielding properties of wood powder.

Building on this research background, the present study employs a synergistic doping modification strategy combining fly ash and TiO_2. By leveraging the stability of SiO_2 in fly ash and the strong ultraviolet absorption capacity of TiO_2, along with the active free radicals generated, we aim to produce wood powder-based composite materials with enhanced stability and light oxidation resistance while carefully controlling the addition of the materials. The microscopic morphology, bonding structure, and performance enhancement mechanisms of the composite material were analyzed using scanning electron microscopy (SEM), X-ray photoelectron spectroscopy (XPS), Fourier-transform infrared spectroscopy (FTIR), and UV–Vis spectroscopy. Finally, the wood flour-based composite material was fabricated into a garden outdoor chair to explore its practical application, providing theoretical support for the use of wood flour in outdoor furniture and the development of green, environmentally friendly products.

2. Materials and Methods

2.1. Experimental Raw Materials

The materials and drugs used in this experiment include fly ash (SiO_2, Al_2O_3, Fe_2O_3, MgO), wood flour (poplar powder, particle size 30 μm, purchased from Shandong Province, China), H_2SO_4 (98%, Sinopharm Reagent, Beijing, China), C_2H_5OH (AR, Sinopharm Reagent, Beijing, China), C_4H_8O (THF, Aladdin, Shanghai, China), EP (Toughened epoxy resin, Sinopharm Reagent, Beijing, China), TiO_2 (Spherical particles of white powder, >99%, Aladdin, Shanghai, China), PA (Aladdin, Shanghai, China), and PET (Aladdin, Shanghai, China). All reagents were of analytical grade and used directly without further purification.

2.2. Preparation of Wood Flour-Based Composite Materials

2.2.1. Pretreatment of Fly Ash

Because fly ash contains a high concentration of metallic impurities, it must be treated for harmlessness before composite material preparation. An appropriate amount of fly ash is placed in a 1.5 mol/L sulfuric acid solution with a solid-to-liquid ratio of 1:6. The mixture is then stirred at room temperature for 2 h and filtered to obtain a residue. The filtered fly ash is then washed three times with anhydrous ethanol, oven-dried at 60 °C for 12 h, and ground to a 200-mesh size for later use.

2.2.2. Preparation of Wood Flour–Fly Ash-TiO_2

Preparation of the wood flour–fly ash material: 8 g of wood flour was weighed and placed in a beaker. 200 mL of tetrahydrofuran and 3 g of treated fly ash were then added to the beaker and ultrasonically dispersed for 10 min. The mixture was then heated to 70 °C in a water bath and stirred for 8 h to obtain a wood flour-modified dispersion. The resulting dispersion was centrifuged at 5000 rpm for 10 min, washed and centrifuged three times, and dried to obtain the wood flour–fly ash composite material.

Preparation of the wood flour–fly ash–TiO_2 material: Weigh 22 g of epoxy resin into a beaker, add the resulting wood flour–fly ash composite, and add 0.5% TiO_2 by mass. Also, add 5 g of polyamide as a curing agent. After stirring thoroughly, place the mixture into a mold, shake repeatedly on a shaker, and let it stand at room temperature for 24 h to cure before demolding. This process was repeated three times, varying the TiO_2 content for comparative experiments: 0%, 1%, and 1.5%. The summary table of the formulations and experimental flow is shown in Table 1 and Figure 1.

Table 1. Summary table of the formulations.

Materials	Fly Ash	Wood Flour	TiO_2	Epoxy Resin	Polyamide
0% TiO_2	3 g	8 g	0% wt	22 g	5 g
0.5% TiO_2	3 g	8 g	0.5% wt	22 g	5 g
1.0% TiO_2	3 g	8 g	1.0% wt	22 g	5 g
1.5% TiO_2	3 g	8 g	1.5% wt	22 g	5 g

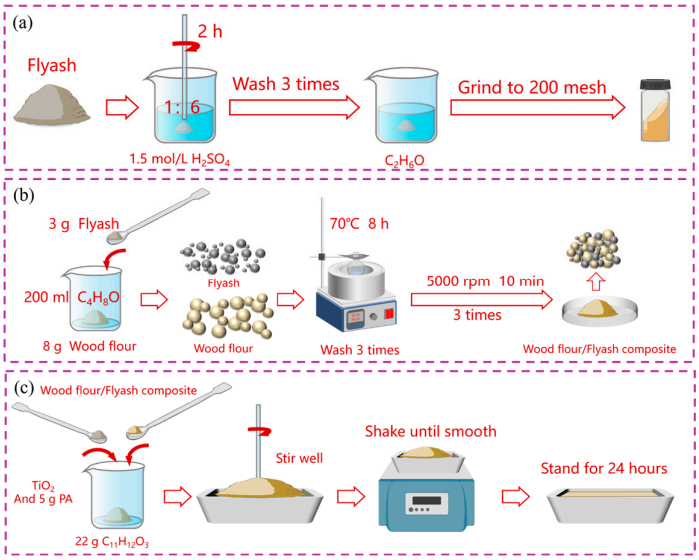


Figure 1. Flowchart of preparation of wood powder-based composite materials. (**a**) Pretreatment of Fly Ash. (**b**) The mixture of Flyash and Wood flour. (**c**) The synthesis of Wood flour/Flyash composite.

2.3. Material Analysis

Scanning electron microscopy (SEM, Hitachi Regulus 8100, Tokyo, Japan) was used to characterize the microstructure of the wood powder-fly ash-TiO_2 composites and observe the micromorphology of the composites after loading with fly ash and TiO_2. X-ray photoelectron spectroscopy (XPS, PHI-5000versaprobe III, Tokyo, Japan) was used to analyze the bonding structure and binding energy changes of Ti, O, and Si elements in the materials. Fourier transform infrared spectroscopy (Nicolet Nexus 470, Madison, WI, USA) was used to analyze changes in the molecular structure and groups on the material surface. The spectral resolution was 0.4 cm^{-1}, and the scanning range was 400–4000 cm^{-1}. Ultraviolet–visible spectrophotometry (UV) and thermogravimetric analysis (TGA) were used to analyze the UV resistance and thermal stability of the composite material. The UV scanning range was 200–800 nm. The TGA test was performed at a temperature range of 30–800 °C at a rate of 10 °C/min in a nitrogen atmosphere. The hydrophobicity of the material was tested using a water contact angle test, using pure water as the test solution.

3. Results and Discussion

3.1. Analysis of Structure and Performance of Wood Flour-Based Composite Materials

The microscopic morphology of the prepared wood powder-based composite materials was analyzed using scanning electron microscopy (SEM, Hitachi Regulus 8100, Hitachi, Tokyo, Japan). The results indicate that the surfaces of all four samples exhibited slight agglomeration (Figure 2); however, the overall structure remained relatively dense. The sample without TiO_2 showed numerous internal pores. This occurrence can be attributed to uneven local liquid dispersion caused by the small fly ash particles during the stirring process, as well as the bubbles generated during mixing. As the TiO_2 content increased, the number of pores within the material gradually decreased, and the pore size also diminished. This improvement is due to the excellent dispersibility of TiO_2, which facilitates a more uniform distribution of fly ash and effectively suppresses bubble formation. Additionally, TiO_2 fills the voids, thereby reducing the internal stress of the material, increasing the interaction force at the contact surfaces, and enhancing both the strength and stability of the composite material's internal structure. Consequently, the addition of a small amount of TiO_2 results in a structurally stable wood powder-based composite material, thereby improving its service life and suitability for outdoor applications.

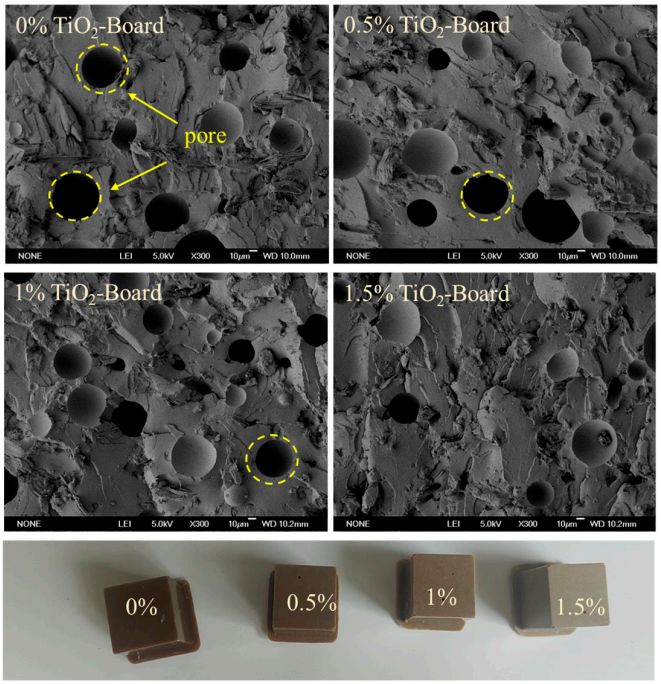


Figure 2. Microstructure and sample picture of wood powder based composite materials.

Subsequently, X-ray photoelectron spectroscopy (XPS) tests were conducted on the wood powder-based composite material to investigate changes in the internal bonding structure during the TiO_2 modification process. The results are presented in Figure 3. Peak fitting of the Si 2p orbital (Figure 3a) reveals that, in the absence of TiO_2, a characteristic peak of binding energy appears at 103.67 eV, attributed to the Si-O bond. This indicates that a small amount of SiO_2 in the fly ash is combined with the wood powder. Upon the addition of 0.5% TiO_2, a new characteristic peak at 105.18 eV emerges, corresponding to the Si-O-Ti bond (silicon–titanium linkages that enhance structural integrity). As the TiO_2 content increases, the Si-O bond gradually shifts to a lower binding energy position, while the Si-O-Ti bond shifts to a higher binding energy position, with the peak area increasing. This suggests that the electron cloud density increases. The additional electrons in SiO_2 will have a stronger shielding effect on the inner layer electrons, weakening the attraction of

the atomic nucleus to the inner layer electrons and enhancing electron transfer. Indicating charge transfer on the Si-O surface and the formation of more Si-O-Ti bonds [34,35], which enhances the structural strength of the wood powder-based composite material. The narrow spectrum analysis of the Ti 2p orbital shows that the Ti 2p orbital splits into two components: Ti $2p_{1/2}$ and Ti $2p_{3/2}$ (Figure 3b). For the sample with 0.5% TiO_2, two characteristic peaks appear at 455.61 eV and 461.34 eV, with a binding energy difference of 5.73 eV attributed to TiO_2 [35]. As the amount of TiO_2 increases, the binding energy difference of the prepared wood powder-based composites remains essentially unchanged, indicating that the TiO_2 and wood powder are well mixed and evenly dispersed. The high-resolution XPS spectrum of the O 1s orbital is shown in Figure 3c. In the absence of TiO_2, peak fitting reveals two characteristic peaks at binding energies of 529.12 eV and 530.83 eV, corresponding to lattice oxygen (O_L, Si-O and Ti-O) and free -OH, respectively. With increasing TiO_2 content, the -OH group shifts toward higher binding energies, and the peak area gradually decreases, enhancing the material's hydrophobicity, this is because the holes inside TiO_2 particles adsorb the -OH reaction in the lignin structure of water. Simultaneously, a characteristic peak appears at 530.59 eV, attributed to adsorbed oxygen (O_A). TiO_2 is a typical n-type semiconductor with a large bandgap of approximately 3.2 eV. It reacts with surface adsorbed substances such as water and oxygen, causing electrons to rapidly migrate to the surface of titanium dioxide particles, generating numerous active free radicals that enhance the antioxidant and UV resistance of the wood powder-based composite, thereby improving its durability in outdoor environments.

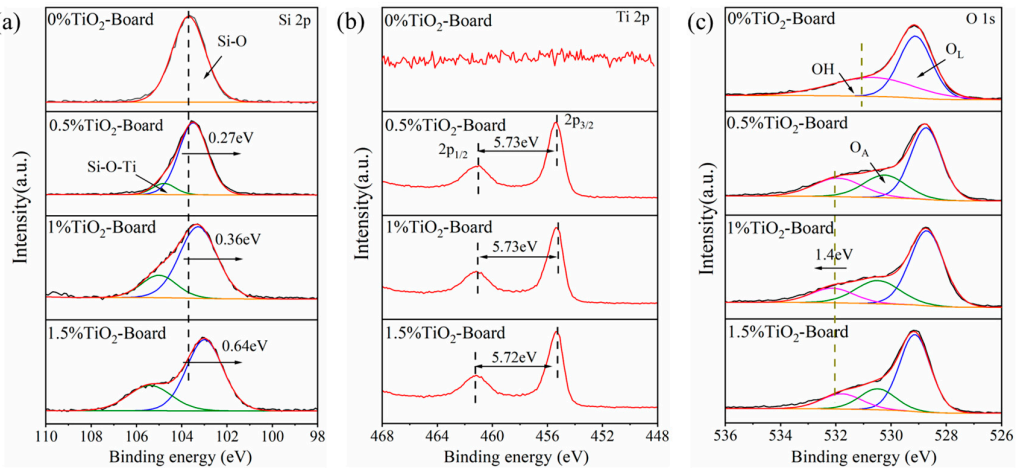


Figure 3. High-resolution XPS spectra of wood powder-based composites: (**a**) Si 2p orbital, (**b**) Ti 2p orbital, (**c**) O 1s orbital.

To further investigate the changes in the molecular structure of the composite material during the TiO_2 modification process, particularly regarding the bonding modes and functional groups of wood powder, TiO_2, and polyamide, infrared spectroscopy analysis was performed, with the results depicted in Figure 4a. The infrared spectrum of pure phase wood powder shows an absorption peak at a wavelength of 3368.2 cm^{-1}, which corresponds to the stretching vibration of hydroxyl (-OH) groups in structural water. The absorption peak of fly ash at 1102.8 cm^{-1} is attributed to the bending vibration of Si-O bonds, while the peak for TiO_2 at 689.9 cm^{-1} corresponds to the vibration of Ti-O bonds. In the TiO_2-Board (1.5%), a stretching vibration peak for -CO-NH- appears at 1181.4 cm^{-1}, and -CH_2 bonds form at wavelengths of 2856.5 cm^{-1} and 2927.9 cm^{-1}. This is due to the reaction between polyamide and lignin in the wood powder, resulting in the formation of ester bonds, which enhances the structural strength of the composite material. A sharp Si-O-Si absorption peak appears at 1031.7 cm^{-1}, indicating that the SiO_2 in the fly ash

reacts with the -OH groups in the wood powder to form a more stable Si-O-Si structure, thereby strengthening the interaction between the materials. Furthermore, the addition of TiO_2 weakens the peak intensity of free hydroxyl groups (-OH), effectively inhibiting water absorption and improving the hydrophobicity of the composite material, which aligns with the XPS findings.

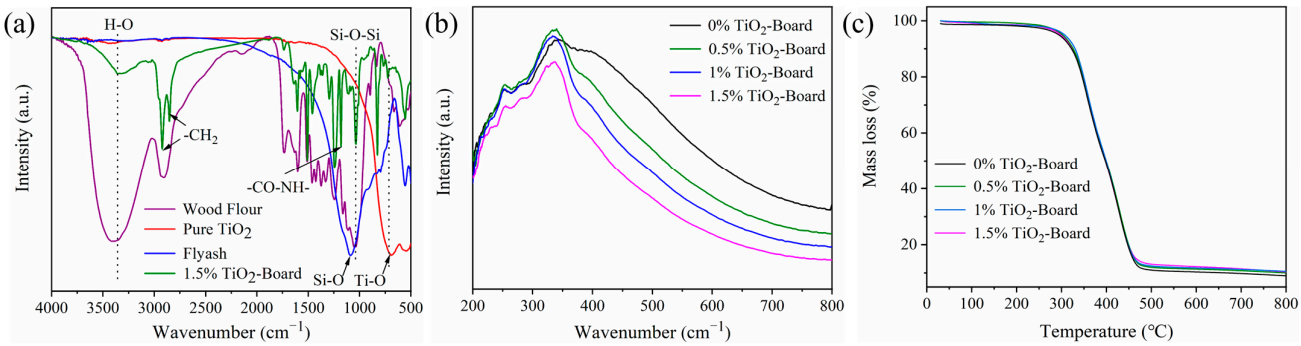


Figure 4. (**a**) FTIR spectrum, (**b**) UV–visible absorption spectrum, and (**c**) thermogravimetric curve of wood powder-based composite materials.

Outdoor furniture is subject to prolonged exposure to ultraviolet radiation. To evaluate the shielding ability against UV rays, we measured the average absorbance of the prepared composite material at wavelengths ranging from 200 to 800 nm. Figure 4b shows the ultraviolet–visible light absorption spectrum of the material with varying TiO_2 content. The 0% TiO_2-Board partially absorbs UV light in the 275–300 nm range, attributable to the large amount of lignocellulose in wood flour, which contains numerous free and etherified phenolic hydroxyl groups with a UV absorption peak at 280–290 nm. Thus, wood flour possesses a certain degree of UV absorption capacity. When TiO_2 is added, the composite material's UV absorption effect in the 275–300 nm range remains similar, indicating that the addition of TiO_2 does not significantly alter the UV absorption for UVB (275–320 nm). However, compared to the material without TiO_2, the UV absorption peak of the composite material in the 325–400 nm range becomes noticeably narrower with the addition of TiO_2. This is because TiO_2 is a wide bandgap semiconductor that can absorb photons with wavelengths less than or equal to 387 nm (corresponding to ultraviolet light). This is because TiO_2 acts as a filler and photocatalyst, reducing porosity and generating active radicals that improve UV resistance [36]. Additionally, TiO_2 exhibits a high refractive index and strong scattering and reflection capabilities for ultraviolet rays (particularly UVA and UVB), contributing to the excellent UV resistance of the composite material.

Figure 4c displays the thermogravimetric curves of the four samples. It is evident that all four materials experience slight mass loss from 0 to 200 °C, primarily due to the evaporation of water within their internal structure. As the temperature rises above 300 °C, a significant mass loss rate is observed, mainly attributed to the thermal decomposition of organic matter such as phenolic hydroxyl groups and benzene rings in the wood cellulose present in the wood powder. Concurrently, the large-scale decomposition of epoxy resin at 350 °C accelerates the material loss rate. All materials reach a stable state at approximately 450 °C. At 500 °C, the sample without TiO_2 exhibits the lowest residual mass fraction, approximately 11.6%. In contrast, after adding TiO_2, the residual mass fractions of the composites remain similar, reaching 13.4% for the 1.5% TiO_2-Board. This suggests that the addition of a small amount of TiO_2 has a minimal effect on the thermal stability of the composite; however, the overall stability is improved.

Natural wood powder contains a significant amount of phenolic hydroxyl groups and structural water, along with numerous pores, which leads to its high water absorp-

tion capacity. This characteristic makes it susceptible to mold and corrosion in humid environments, severely affecting its service life. To evaluate the waterproof ability of the sample, the prepared material was tested for contact angle and the physical ruler is 2 mm, the results are shown in Figure 5. The water contact angle of the material without TiO_2 is approximately 85.7°. This can be attributed to the reaction between polyamide, fly ash, and cellulose in the wood powder, which forms -CO-NH- and Si-O-Si bonds, thereby reducing the amount of free -OH groups in the material. Additionally, the epoxy resin enhances hydrophobic properties after curing. Following the addition of TiO_2, the water contact angle of the composite material gradually increased, reaching 100.6° for the 1.5% TiO_2-Board composite, further enhancing its hydrophobicity. This improvement is due to TiO_2 effectively filling the pores within the composite material and forming stable Si-O-Ti bonds on the surface, which reduces water penetration and enhances the waterproofing properties of outdoor furniture.

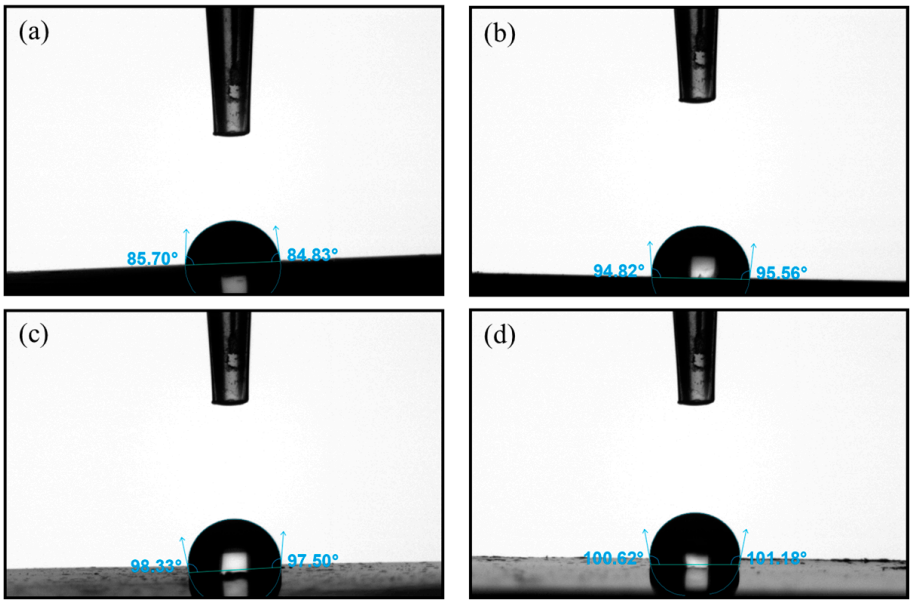


Figure 5. Contact angle test of wood powder-based composites (**a**) 0% TiO_2-Board, (**b**) 0.5% TiO_2-Board, (**c**) 1% TiO_2-Board, (**d**) 1.5% TiO_2-Board.

The compressive strength of the four composite materials was also tested, four compressive strength tests were conducted on each sample, and the average value was taken, and the standards followed GB, with the results presented in Figure 6. The compressive strength of the material without TiO_2 is 62.1 MPa, exceeding that of 32.5R cement by 32.5 MPa. Compared to Novosel et al. [17], our composite achieved a 10% higher compressive strength with less filler content. This enhancement is due to the small amount of SiO_2 in the fly ash, which forms stronger Si-O-Si bonds with lignin. Upon adding a certain amount of TiO_2, the compressive strength of the material gradually increased, with the 1.5% TiO_2-Board achieving the highest compressive strength of approximately 69.8 MPa. This improvement is attributed to the excellent dispersibility of TiO_2, which inhibits bubble formation, reduces internal porosity in the material, and enhances overall strength. Furthermore, the addition of TiO_2 results in the formation of Si-O-Ti bonds, improving the mechanical properties of the material and extending the lifespan of outdoor furniture.

To further assess the waterproof ability of the material, the sample was immersed in water for 98 h, and its mass was recorded every 12 h. The water absorption curve is depicted in Figure 7. All four materials experienced a slight increase in mass during the test, with the 0% TiO_2-Board exhibiting the greatest increase, from 15.27 g to 15.42 g, reflecting

a weight gain of approximately 0.98%. As the TiO_2 content increased, the composite's water absorption gradually decreased. After 98 h of immersion, the weight gains for the 0.5% TiO_2-Board, 1% TiO_2-Board, and 1.5% TiO_2-Board were 0.63%, 0.39%, and 0.33%, respectively. This indicates that the addition of TiO_2 enhances the composite's water repellency, consistent with the previous water contact angle test results.

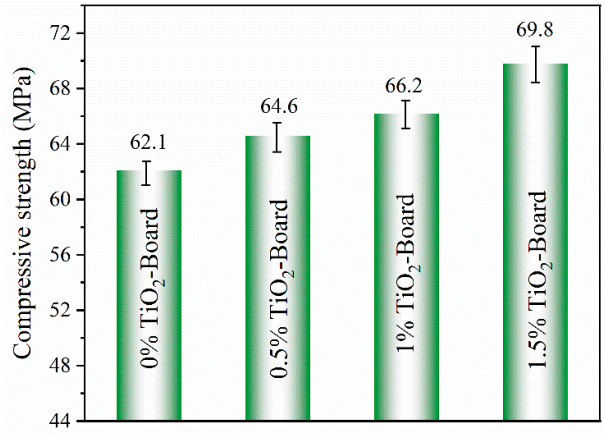


Figure 6. Compressive strength of wood flour-based composites.

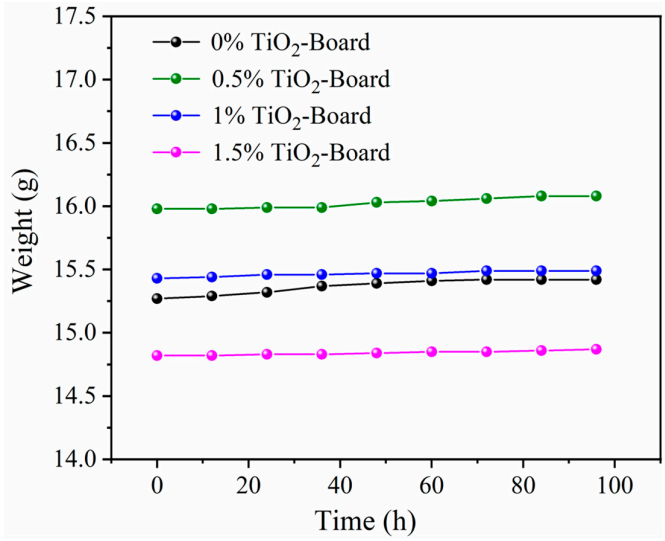


Figure 7. Water absorption curve of wood powder-based composite materials.

3.2. The Application of Wood Powder-Based Composites in the Design of Outdoor Garden Benches

The primary function of outdoor garden seating is to provide resting spaces for pedestrians and visitors in public areas. Different scenarios necessitate various sizes, styles, and functionalities. Rust-resistant materials such as aluminum alloy, stainless steel, and waterproof paint are recommended for use in humid and rainy conditions, while UV-resistant materials like HDPE woven fabric are suited for areas exposed to direct sunlight. Moreover, to better serve users, outdoor seating designs must meet specific requirements: comfort, ergonomics, structural stability, a smooth, non-angular surface, safety, and ease of maintenance and cleaning. Common seating materials like teak offer natural beauty and corrosion resistance but can be expensive and require regular maintenance. Metal materials, such as aluminum alloy and stainless steel, are durable and rust-resistant but may feel cold in winter. Therefore, designing chairs that combine wood powder-based composite materials with metal elements can provide the aesthetic texture of wood while ensuring the stability of metal components. Finally, aesthetics should not be overlooked; the

chairs should harmonize with the overall style of the garden landscape design, adhere to ecological protection principles, and feature smooth and unobtrusive curves to complement the natural surroundings. These improvements suggest that the composite can significantly extend the lifespan of outdoor furniture in humid and high-UV environments.

3.2.1. Design Analysis

(1) Seat design:

Based on the above experimental analysis, a wood flour-based composite material prepared with a TiO_2 addition of 1.5% exhibits excellent UV and water resistance. Therefore, this material was selected to create the seat of the modular outdoor garden chair (Figure 8). The smallest unit of the modular outdoor garden chair is a 380 mm × 380 mm × 50 mm square. The design process adhered to the principles of simplicity, comfort, and ergonomics. PET was selected as the mold filler for the seat due to its clean, environmentally friendly, non-toxic, odorless, smooth surface, and heat resistance, making it easy to use and modularize.

(2) Seat leg design:

The legs are made of 316 stainless steels, which is resistant to atmospheric oxidation and corrosion. They are strong enough to withstand humid and coastal environments. The legs are 50 mm × 80 mm in cross-section and 450 mm in length. To improve corrosion resistance, the stainless steel is coated with an anti-corrosion paint, and the bottom of the legs is affixed with rubber for added anti-slip and wear resistance.

(3) Connection method:

The stainless-steel legs are connected by welding, and the seat surface made of composite material is overlapped on the stainless-steel frame and can be fixed with screws by punching.

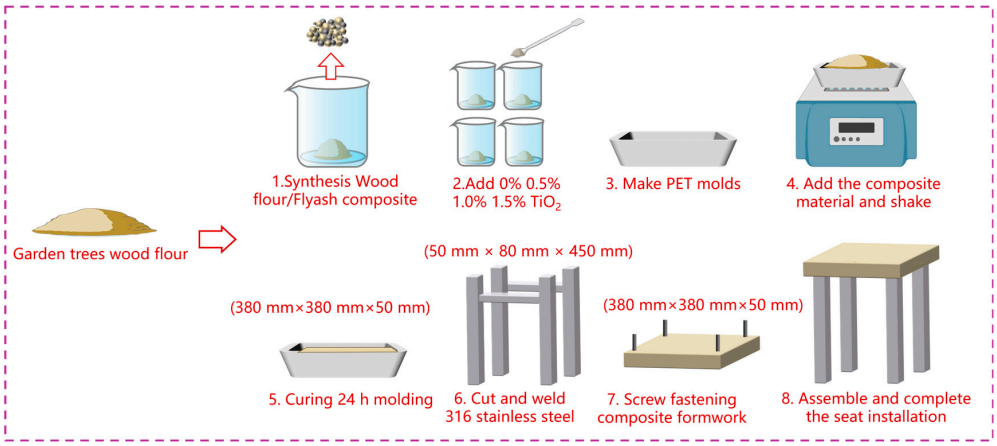


Figure 8. Seat production flow chart.

3.2.2. Seat Performance Analysis

Long-term use of outdoor chairs can lead to stability changes, discoloration due to ultraviolet rays, and internal corrosion caused by rain. Therefore, after preparing wood powder-based composite materials into outdoor chairs, their performance needs to be analyzed to ensure their optimal suitability for practical environments, focusing on weighing stability, water resistance, and safety. These multi-dimensional tests allow for a comprehensive assessment of the long-term practicality of outdoor chairs, ensuring their safety and durability in various environments. This provides valuable in-

sights into the application and promotion of wood powder-based composite materials in outdoor furniture.

(1) Stability Test

To evaluate the stability of modular garden outdoor chairs made from wood powder-based composite materials, this experiment tested and analyzed the chairs' load-bearing capacity, overall structural integrity, and mechanical stability. A weight of approximately 200 kg was placed on the chair for two days to assess load-bearing capacity and structural stability, and place the chair in an outdoor environment to simulate human use of the outdoor seat, Changes in the chair's length, width, and height were recorded every 12 h during the test, while the seat was observed for any bending, deformation, or fracture. The results are presented in Table 2. The findings indicate that the chair's dimensions remained unchanged, and no fractures occurred, thereby maintaining overall structural stability. This demonstrates that the chair is suitable for a variety of outdoor environments and possesses a high structural strength that meets the demands of daily use.

Table 2. Dimensional changes of chairs during load-bearing test.

Experiment	Length (mm)	Width (mm)	Height (mm)
0 h	380	380	500
12 h	380	380	500
24 h	380	380	500
36 h	380	380	500
48 h	380	380	500

Outdoor garden seating is often exposed to humid environments such as southern China, coastal areas, and regions with extreme rainfall, necessitating a certain level of waterproofing. To simulate heavy rain conditions, wood boards made from wood powder-based composite materials were immersed in water for 98 h. Fully immerse the seat surface in water, using tap water for testing, simulating an environment soaked in heavy rain. The weight of the boards was recorded every 12 h, and the total weight change before and after immersion was noted to assess any surface expansion, deformation, or instances of paint peeling or discoloration. The results are illustrated in Figure 9. After being soaked in water for 98 h, the size of the chair seat remained unchanged, and no fading or surface peeling was observed during the experiment. In addition, the mass increased from 2.81 kg to 2.82 kg before and after soaking, with a weight gain of approximately 0.36%. This indicates that the wood powder-based composite material, prepared by synergistically doping fly ash and TiO_2, possesses excellent waterproof properties and is suitable for use in humid and rainy outdoor environments.

(2) Safety Performance Test—Harmful Substance Detection

Due to the high organic content and wood cellulose in the prepared outdoor garden chairs, safety testing was conducted to ensure their environmental friendliness. The chairs were placed in a confined space for 48 h, during which the formaldehyde content in the air and the phthalate content in the chairs were measured every 12 h. The room size is about 10 m^2, and there are no furniture or formaldehyde absorbing green plants in the room. Formaldehyde testing method: Use a formaldehyde detection box for testing. Open the self-test box and let it sit in a closed space for 30 min to allow formaldehyde in the air to react with the absorbent. Subsequently, quickly pour the color developer into the absorption box and gently shake it to mix evenly, allowing it to fully develop color. And compare it with the standard color chart to find the closest color, and the corresponding value is the approximate range of formaldehyde concentration. Phthalate testing method:

Cut small fragments from the chair, place them in methanol, and dissolve phthalates from the sample into the solvent using ultrasound. After appropriate dilution and filtration, the extract was analyzed by gas chromatography-mass spectrometry (GC-MS). By comparing the characteristic peaks of phthalates in the test sample with the retention time and mass spectrum of the standard, the content of phthalates in the chair can be confirmed.

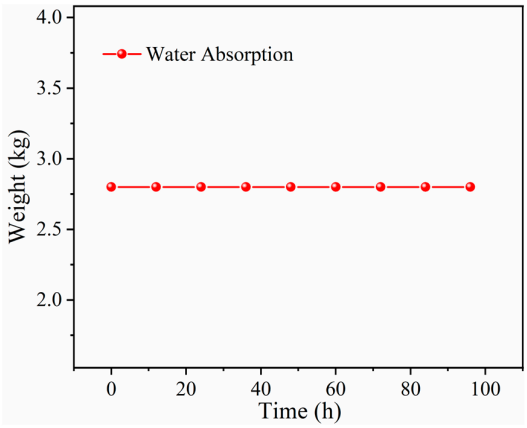


Figure 9. Mass change curve of chair panel after being immersed in water.

The results are shown in Figure 10. The experimental results indicated that after 48 h, the indoor formaldehyde content in the chair was approximately 0.03 mg/m^3, which complies with the GB50325-2020 standard (0.08 mg/m^3) [37]. Additionally, the phthalate content in the chair was measured at 219 ppm, adhering to the standards for plastic products outlined in GB 24613-2009 (<0.1%, or 1000 ppm) [38]. These findings confirm that chair materials made from fly ash, TiO_2, and wood flour are environmentally friendly and safe, presenting no harm to human health and making them suitable for widespread outdoor use. In addition, life-cycle assessment (LCA) of materials is also necessary in subsequent work [39], which is an important indicator for evaluating material performance.

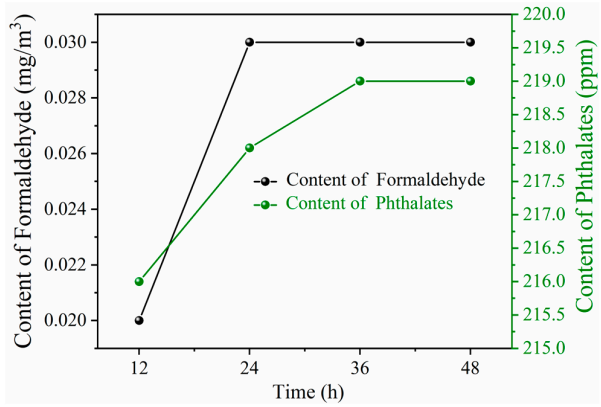


Figure 10. Formaldehyde and phthalate test curves.

4. Conclusions

In this study, wood flour was modified through the synergistic doping of fly ash and TiO_2 to create a high-strength wood flour composite with excellent oxidation resistance, water resistance, and UV resistance. The composite was then applied to outdoor seating design. Based on the results and discussions presented, the following conclusions were drawn:

(1) Structural strength and stability: Mechanical Strength: Scanning electron microscopy (SEM) and X-ray photoelectron spectroscopy (XPS) tests revealed that the composite material

exhibited exceptional performance across all criteria when the TiO_2 content reached 1.5%. As the TiO_2 content increased to 1.5%, more stable Si-O-Si and Si-O-Ti bonds were formed, enhancing the material's structural strength and dimensional stability.

(2) UV Resistance and hydrophobicity: As the amount of TiO_2 added increased, a large amount of reactive free radicals (O_A) were generated and the free -OH groups in the composite material decreased, effectively improving the UV resistance and moisture penetration inhibition of composite materials. The surface water contact angle gradually increased, reaching 100.6° for the 1.5% TiO_2-Board, significantly improving its hydrophobicity. This enhanced waterproof characteristic will increase the application potential of outdoor seating in humid and rainy environments.

(3) Application in furniture design: The 1.5% TiO_2 composite demonstrated optimal performance in strength, UV resistance, and hydrophobicity, validating its suitability for outdoor furniture and enabling its use for the design of outdoor chairs. Actual testing demonstrated excellent structural stability and waterproof performance. Moreover, safety testing confirmed that the chair's formaldehyde and phthalate emissions met national safety standards, ensuring its environmental safety for outdoor use.

This study aims to develop a high-performance wood flour composite using fly ash and TiO_2, targeting improved mechanical strength, UV resistance, and hydrophobicity for outdoor furniture applications. This strategy provides a new approach to modifying wood flour-based materials for outdoor garden furniture and addresses the issue of solid waste disposal generated by landscaping materials to a certain extent. The findings of this study highlight the potential applications of modified wood flour in outdoor garden furniture and sustainable material innovation. Future studies should explore long-term weathering effects, biodegradability, and scaling up production for commercial applications.

Author Contributions: Conceptualization, H.Z. and Y.G.; Methodology, K.Z.; Software, Y.G.; Resources, K.Z.; Data curation, H.Z.; Writing—original draft, Y.G.; Writing—review and editing, K.Z.; Supervision, K.Z.; Visualization, K.Z.; Funding acquisition, K.Z., H.Z. and Y.G. are co first authors, they contributed equally to this work. All authors have read and agreed to the published version of the manuscript.

Funding: The authors declare that no funds, grants, or other support were received during the preparation of this manuscript.

Institutional Review Board Statement: Not applicable.

Informed Consent Statement: Not applicable.

Data Availability Statement: Data are contained within the article.

Conflicts of Interest: The authors declare no conflicts of interest.

References

1. Alam, M.M.; Greco, A.; Rajabimashhadi, Z.; Corcione, C.E. Efficient and environmentally friendly techniques for lignocellulosic biomass processing. *Clean. Mater.* **2024**, *13*, 100253. [CrossRef]
2. Upton, B.M.; Kasko, A. Biomass-Derived Poly(ether-amide)s Incorporating Hydroxycinnamates. *Biomacromolecules* **2019**, *20*, 758–766. [CrossRef] [PubMed]
3. Ralph, J.; Lapierre, C.; Boerjan, W. Lignin structure and its engineering. *Curr. Opin. Biotechnol.* **2019**, *56*, 240–249. [CrossRef] [PubMed]
4. Gioia, C.; Colonna, M.; Tagami, A.; Medina, L.; Sevastyanova, O.; Berglund, L.A.; Lawoko, M. Lignin-Based Epoxy Resins: Unravelling the Relationship between Structure and Material Properties. *Biomacromolecules* **2020**, *21*, 1920–1928. [CrossRef]
5. Li, J.M.; Zhang, Z.Y.; Zhang, Y.; Sun, F.L.; Wang, D.Y.; Wang, H.; Jin, Z.F. Synergistic effect of lignin and ethylene glycol crosslinked epoxy resin on enhancing thermal, mechanical and shape memory performance. *Int. J. Biol. Macromol.* **2021**, *192*, 516–524. [CrossRef]

6. Zhang, W.L.; Qiu, X.Q.; Wang, C.W.; Zhong, L.; Fu, F.B.; Zhu, J.H.; Zhang, Z.J.; Qin, Y.L.; Yang, D.J.; Xu, C.C. Lignin derived carbon materials: Current status and future trends. *Carbon Res.* **2022**, *1*, 14. [CrossRef]
7. Camargos, H.M.C.; Yang, L.; Jackson, J.C.; Tanganini, I.C.; Francisco, K.R.; Ceccato-Antonini, S.R.; Rezende, C.A.; Faria, A.F. Lignin and Nanolignin: Next-Generation Sustainable Materials for Water Treatment. *ACS Appl. Bio Mater.* **2025**, *8*, 2632–2673. [CrossRef]
8. Suvanjumrat, C.; Chansoda, K.; Chookaew, W. Additive manufacturing advancement through large-scale screw-extrusion 3D printing for precision parawood powder/PLA furniture production. *Clean. Eng. Technol.* **2024**, *20*, 100753. [CrossRef]
9. Candelier, K.; Thevenon, M.F.; Petrissans, A.; Dumarcay, S.; Gerardin, P.; Petrissans, M. Control of wood thermal treatment and its effects on decay resistance: A review. *Ann. For. Sci.* **2016**, *73*, 571–583. [CrossRef]
10. Fan, Y.F.; Zhu, Z.Q.; Luan, J.C.; Liu, Y. Exploring the Application Method of Bamboo Powder in Promoting the Development of Sustainable Outdoor Furniture. *Sustainability* **2024**, *16*, 11282. [CrossRef]
11. Ditommaso, G.; Gaff, M.; Kačík, F.; Sikora, A.; Sethy, A.; Corleto, R.; Razaei, F.; Kaplan, L.; Kubš, J.; Das, S.; et al. Interaction of technical and technological factors on qualitative and energy/ecological/economic indicators in the production and processing of thermally modified merbau wood. *J. Clean. Prod.* **2020**, *252*, 119793. [CrossRef]
12. Zhang, N.; Mao, Y.Q.; Wu, S.S.; Xu, W. Effects of the ball milling process on the particle size of graphene oxide and its application in enhancing the thermal conductivity of wood. *Forests* **2022**, *13*, 1325. [CrossRef]
13. Zelinka, S.L.; Altgen, M.; Emmerich, L.; Guigo, N.; Keplinger, T.; Kymäläinen, M.; Thybring, E.E.; Thygesen, L.G. Review of Wood Modification and Wood Functionalization Technologies. *Forests* **2022**, *13*, 1004. [CrossRef]
14. Hill, C.; Altgen, M.; Rautkari, L. Thermal modification of wood—a review: Chemical changes and hygroscopicity. *J. Mater. Sci.* **2021**, *56*, 6581–6614. [CrossRef]
15. Donath, S.; Militz, H.; Mai, C. Wood modification with alkoxysilanes. *Wood Sci. Technol.* **2004**, *38*, 555–566. [CrossRef]
16. Mosadeghzada, Z.; Ahmad, I.; Daika, R.; Ramli, A.; Jajaludin, Z. Preparation and properties of acacia sawdust/UPR composite based on recycled PET. *Malays. Polym. J.* **2009**, *4*, 30–41.
17. Novosel, A.; Sedlar, T.; Čizmar, D.; Turkulin, H.; Živković, V. Structural reinforcement of bi-directional oak-wood lamination by carbon fibre implants. *Constr. Build. Mater.* **2021**, *287*, 123073. [CrossRef]
18. Mathapati, M.; Amate, K.; Prasad, C.D.; Jayavardhana, M.L.; Raju, T.H. A review on fly ash utilization. *Mater. Today Proc.* **2022**, *50*, 1535–1540. [CrossRef]
19. Zygmunt-Kowalska, B.; Pielichowska, K.; Trestka, P.; Ziąbka, M.; Kuźnia, M. The effect of ash silanization on the selected properties of rigid polyurethane foam/coal fly ash composites. *Energies* **2022**, *15*, 2014. [CrossRef]
20. Nayl, A.A.; Abd-Elhamid, A.I.; Aly, A.A.; Bräse, S. Recent progress in the applications of silica-based nanoparticles. *RSC. Adv.* **2022**, *12*, 13706–13726. [CrossRef]
21. Cao, M.T.; Tang, M.W.; Lin, W.S.; Ding, Z.H.; Cai, S.; Chen, H.X.; Zhang, X.X. Facile Fabrication of Fluorine-Free, Anti-Icing, and Multifunctional Superhydrophobic Surface on Wood Substrates. *Polymers* **2022**, *14*, 1953. [CrossRef] [PubMed]
22. Petrillo, M.; Sandak, J.; Grossi, P.; Sandak, A. Chemical and appearance changes of wood due to artificial weathering—Dose–response model. *J. Near Infrared Spec.* **2019**, *27*, 26–37. [CrossRef]
23. Carvalho, P.G.; Naveira, R.I.; Granone, L.I.; Mendive, C.B.; Massa, A.E.; Churio, M.S. A comparative review of natural and synthetic UV filters: Gadusol and benzophenone-3 as representative examples. *Environ. Adv.* **2023**, *13*, 100404. [CrossRef]
24. Racovita, A.D. Titanium dioxide: Structure, impact, and toxicity. *Int. J. Environ. Res. Public Health* **2022**, *19*, 5681. [CrossRef]
25. Cole, C.; Shyr, T.; Ou-Yang, H. Metal oxide sunscreens protect skin by absorption, not by reflection or scattering. *Photodermatol. Photoimmunol. Photomed.* **2016**, *32*, 5–10. [CrossRef]
26. Kaur, R.; Bhardwaj, S.K.; Chandna, S.; Kim, K.H.; Bhaumik, J. Lignin-based metal oxide nanocomposites for UV protection applications: A review. *J. Clean. Prod.* **2021**, *317*, 128300. [CrossRef]
27. Pánek, M.; Šimůnková, K.; Novák, D.; Dvořák, O.; Schönfelder, O.; Šedivka, P.; Kobetičová, K. Caffeine and TiO_2 Nanoparticles Treatment of Spruce and Beech Wood for Increasing Transparent Coating Resistance against UV-Radiation and Mould Attacks. *Coatings* **2020**, *10*, 1141. [CrossRef]
28. Ghamarpoor, R.; Fallah, A.; Jamshidi, M. Investigating the use of titanium dioxide (TiO_2) nanoparticles on the amount of protection against UV irradiation. *Sci. Rep.* **2023**, *13*, 9793. [CrossRef]
29. Bulcha, B.; Tesfaye, J.L.; Anatol, D.; Shanmugam, R.; Dwarampudi, L.P.; Nagaprasad, N.; Bhargavi, V.L.N.; Krishnaraj, R. Synthesis of zinc oxide nanoparticles by hydrothermal methods and spectroscopic investigation of ultraviolet radiation protective properties. *J. Nanomater.* **2021**, *2021*, 8617290. [CrossRef]
30. Sivakumar, K.; Nalini, A. Benzophenone type UVR filters for various materials: A review. *J. Mol. Liq.* **2024**, *395*, 123905. [CrossRef]
31. Grätzel, M. Photoelectrochemical cells. *Nature* **2001**, *414*, 338–344. [CrossRef]
32. Asahi, R.; Morikawa, T.; Ohwaki, T.; Aoki, K.; Taga, Y. Visible-light photocatalysis in nitrogen-doped titanium oxides. *Science* **2001**, *293*, 269–271. [CrossRef]

33. Khan, S.U.M.; Al-Shahry, M.; Ingler, J.W.B. Efficient Photochemical Water Splitting by a Chemically Modified n-TiO_2. *Science* **2002**, *297*, 2243–2245. [CrossRef] [PubMed]
34. Jin, Q.J.; Shen, Y.S.; Sui, G.R.; Tao, X.J.; Pan, Y.C.; Zhu, S.M. Synergistic catalytic removals of NO, CO and HC over CeO_2 modified Mn-Mo-W-Ox/TiO_2-SiO_2 catalyst. *J. Rare Earths* **2018**, *36*, 148–155. [CrossRef]
35. Qin, J.T.; Li, J.; Liu, F.Y.; Zhang, Z.L.; Jiang, L.X. Improving the Electrochemical Stability of $TiMn_2$ Middle-Layer for Oxygen Evolution Anode in Sulfuric Acid Solution by High-Temperature Nitriding. *Adv. Sustain. Syst.* **2024**, *8*, 2400061. [CrossRef]
36. Yang, J.Y.; Dai, J.F.; Liu, X.H.; Fu, S.Y.; Zong, E.M.; Song, P.A. A lignin-based epoxy/TiO_2 hybrid nanoparticle for multifunctional bio-based epoxy with improved mechanical, UV absorption and antibacterial properties. *Int. J. Biol. Macromol.* **2022**, *210*, 85–93. [CrossRef]
37. Wei, W.; Howard-Reed, C.; Persily, A.; Zhang, Y. Standard Formaldehyde Source for Chamber Testing of Material Emissions: Model Development, Experimental Evaluation, and Impacts of Environmental Factors. *J. Environ. Sci. Technol.* **2013**, *47*, 14. [CrossRef]
38. Silva, M.J.; Reidy, J.A.; Samandar, E.; Herbert, A.R.; Needham, L.L.; Calafat, A.M. Detection of phthalate metabolites in human saliva. *Arch. Toxicol.* **2005**, *79*, 647–652. [CrossRef]
39. Rizwan, V.; Ibrahim, S.M.; Zaheer, M.M. Explainable artificial intelligence-based compressive strength optimization and Life-Cycle Assessment of eco-friendly sugarcane bagasse ash concrete. *Environ. Sci. Pollut. Res.* **2025**, *32*, 6922–6947. [CrossRef]

Disclaimer/Publisher's Note: The statements, opinions and data contained in all publications are solely those of the individual author(s) and contributor(s) and not of MDPI and/or the editor(s). MDPI and/or the editor(s) disclaim responsibility for any injury to people or property resulting from any ideas, methods, instructions or products referred to in the content.